

# Supplementary Material for “Individual variation in dispersal shapes the fate of pushed vs. pulled range expansions”

Maxime Dahirel, Chloé Guicharnaud, Elodie Vercken

## S1 - Detailed description of the individual-based model in the ODD format

### Purpose and patterns

The model simulates asexual individuals reproducing and dispersing in a linear landscape following an initial introduction, in order to approximate processes at play during natural and experimental range expansions. The aim is to gather insights into how evolutionary dynamics (neutral diversity and dispersal-related traits) and expansion velocity are shaped by trait distribution (means and variances) at the start of the expansion. We specifically focus on traits driving the position of expansions on the pushed/pulled continuum (Birzu et al., 2018, 2019), namely traits shaping the density-dispersal function. Importantly, dispersal and reproduction are stochastic. The focus of the model is on studying the effects of initial trait variation at introduction; as such there is no mutation, for simplicity.

### Entities, state variables and scales

Individuals are haploid and reproduce asexually, and can vary in:

- their location in the landscape ( $x$  coordinate only, since we simulate linear landscapes.  $x$  can only take  $\geq 0$  integer values);
- their dispersal probability  $d$  (real between 0 and 1) and the underlying dispersal traits ( $d_{max}$ ,  $\alpha$ ,  $\beta$ ). Each trait is the (transformed) sum of an additive genetic component ( $a_{[d_{max}]}$ ,  $a_{[\alpha]}$ ,  $a_{[\beta]}$ ) and of a noise/residual part ( $r_{[d_{max}]}$ ,  $r_{[\alpha]}$ ,  $r_{[\beta]}$ ). All these components are reals. See **Initialization** and **Submodels** below for details about the dispersal function;
- the allelic value at a neutral locus  $\gamma$  (binary, 0 or 1);
- their life stage (juvenile or adult, coded as a binary variable);
- their fecundity  $F$  ( $\geq 0$  integer).

We note that the model as it is coded and made available (see **Data availability** in main text) is more general and allows the use of diploid, sexually reproducing individuals, with some slight adaptations in the reproduction submodel. For simplicity we only use and describe the “haploid asexual” scenario here.

Individuals live in discrete patches, which form the spatial units of our model. The model world is one-dimensional, and has closed boundaries. Patches can be described by:

- their location in the landscape ( $x$  coordinate;  $\geq 0$  integer values);
- their population size at the last count  $N$  ( $\geq 0$  integer; population counts occur at points of the cycle where only adults are present);
- their carrying capacity  $K$  ( $\geq 0$  integer;  $K$  is fixed and constant across all patches);

- a series of variables summarizing the trait distributions of the individuals born in the patch (see **Submodels**).

One time step in the model represents one generation of the simulated species' life cycle, and each individual grid cell corresponds to an individual patch. The potentially hostile matrix between patches is abstracted out (there are no "matrix" grid cells) and its effects are summarised in a global environmental variable, dispersal mortality  $m$ . The spatial and temporal extents of the simulations are not fixed and can be set up based on the needs of the simulation experiments.

## Process overview and scheduling

Generations start at the point of the life cycle where only pre-dispersal, pre-reproduction adults are present. The schedule of a generation can be divided in 6 processes: *initial Population count*, *Summary statistics*, *Dispersal*, *second Population count*, *Reproduction*, and *Death*. All individuals and patches must go through one process before the model proceeds to the next. The order in which individuals/patches go through a given process is random.

- *Population count*: Individuals at each patch are counted to update the patch population sizes  $N$  and the neutral allele frequencies for each patch.
- *Summary statistics*: Patches estimate a series of summary variables describing the trait distribution of individuals they currently harbour. This is done because exporting and analyzing individual-level traits would be computationally expensive. A list of the summary variables is provided in **Submodels** below.
- *Dispersal*: Adult individuals may disperse with a probability  $d$  depending on their individual traits ( $d_{max}$ ,  $\alpha$ ,  $\beta$ ) and local population size  $N$  **at the start of the dispersal phase**. The dispersal model is taken from Kun and Scheuring (2006) and described in **Submodels** below. If an individual attempts to disperse, it dies during the attempt with a probability  $m$ . As the model is coded in base Netlogo, which does not include the possibility to directly from Bernoulli or Binomial distributions, a workaround is used. In practice we draw random values from a Uniform(0,1) distribution; if the draw is lower than  $d$  (respectively  $m$ ), the individual disperses (respectively dies). Surviving dispersers are randomly moved to one of the nearest neighbouring patches; that is, the maximal dispersal distance is of 1 patch.
- *Second population count*: The population sizes  $N$  and neutral alleles frequencies at each patch are updated again.
- *Reproduction*: Each remaining adult then produces  $F$  juveniles, with  $F$  drawn from a Poisson distribution and depending on the general growth rate  $r_0$ ,  $K$  and  $N$ . Juveniles are born in the patch currently occupied by their parent (same  $x$ ), and also inherit their genetic values for dispersal-related and neutral loci. Their values for the noise part of the dispersal traits are redrawn at random. The exact fecundity model and inheritance procedures are described in **Submodels** below.
- *Death and end of cycle*: All adults die; juveniles then become adults.

The model then starts the next generation. We chose to make dispersal precede reproduction, so that our model simulates *natal dispersal*, i.e. the movement from birth site to the first reproduction site, arguably the most studied and best understood type of dispersal.

## Design concepts

**Basic principles**: This model follows previous attempts to model evolution in range expansions using an individual-based simulation framework (e.g. Travis et al., 2009), including in the context of pushed expansions (e.g. Erm & Phillips, 2020). This model is a theoretical investigation tool and is not built to make any real-world quantitative prediction, but to develop new qualitative insights about evolutionary dynamics during range expansions. It differentiates itself from previous modelling studies of pushed expansions in an ecological/evolutionary context by:

- the use of a more flexible dispersal function (Kun & Scheuring, 2006).

- a focus on “small” population sizes that are realistic for many “macroscopic” organisms, giving a more important role to discreteness, drift and stochasticity in general, compared to models assuming much larger population sizes either implicitly (e.g. when using continuum models) or explicitly (Birzu et al., 2019).
- the possibility of varying trait heritability, where most models either ignore evolutionary dynamics in focal traits (e.g. Birzu et al., 2019) or assume all variation is genetic (e.g. Erm & Phillips, 2020).

**Emergence:** The number and distribution of individuals and alleles in space are the emergent result of individual dispersal and reproduction, which are stochastic and themselves depend, recursively, on the distribution of individuals in space. Most if not all variables of interest are summaries from these distributions.

**Adaptation:** As population size varies in space and time along the range expansion, dispersal is costly, and fitness is density-dependent (see **Submodels**), dispersal can evolve in an adaptive way in replicates where dispersal traits are heritable.

**Objectives:** There is no direct objective-seeking in this model, in the sense that individuals do not adjust their dispersal behaviour *for* increasing their expected fitness. However, the model allows for evolution; in these cases, natural selection based on differential reproductive success may lead lineages to maximize their reproductive success through time.

**Learning:** Individuals do not learn (see **Sensing**).

**Prediction:** There is no prediction component to individuals’ choices: individuals behave only based on currently available information, including their phenotype.

**Sensing:** In addition to its own trait values, the only information an individual can sense and use is the (last updated) population size  $N$  in the patch it is currently in. Individuals automatically and accurately know  $N$  when needed, and immediately forget it afterwards (there is no memory).

**Interaction:** Individuals do not interact directly with each other. Individuals in the same patch may influence each other indirectly, through the patch population size variable  $N$  which plays a role in both individual dispersal and reproduction.

**Stochasticity:** Dispersal and reproduction are both stochastic. First, for dispersal, the individual probability of dispersing depends on three traits, the values of which are determined stochastically. The genetic components are drawn from Normal distributions at the start of the experiments (and then transmitted deterministically), and the noise components are drawn from Normal distributions at the birth of every individual. Second, once the individual dispersal probability is set, whether or not an individual actually disperses, and whether or not it dies if it disperses, is in effect determined by Bernoulli trials (implemented by determining if a (pseudo-)random number between 0 and 1 is higher or lower than the relevant probability). Finally, the actual fecundity of each individual is a random draw from the relevant Poisson distribution. See **Initialization** and **Submodels** for more details.

**Collectives:** Individuals do not belong to any kind of identifiable social group or collective *per se*. Individuals in the same discrete patch nonetheless influence each other through  $N$  (see **Interaction**).

**Observation:** For memory reasons, it is impractical to save the state of every individual. We instead measure and record patch-level metrics, which convey information about population size, neutral allele frequencies and the means and variances of variables summarizing the dispersal-density functions of individuals born in the patch (see **Submodels**). The user can choose to save these metrics every generation, or for only a subset of generations of interest.

## Initialization

Each expansion starts by creating the landscape (which, as we use nearest-neighbour dispersal, can be any length higher than the number of generations planned for the run), and setting the carrying capacity of all patches to  $K$ . We then introduce  $K$  adult individuals that have not yet dispersed or reproduced to the left-most patch of the landscape ( $x = 0$ ). All other patches are empty. Individual traits and alleles are then initialized as follows:

- the value (0 or 1) at the neutral allele  $\gamma$  is drawn from Bernoulli(0.5) (in practice implemented by randomly selecting an integer between 0 or 1).
- for each dispersal trait  $z$  ( $\text{logit}(d_{max}), \alpha, \beta$ ), the genetic component is drawn from  $\text{Normal}(\bar{z}_{t=0}, \sqrt{h^2 V_{P[z]}})$ , the noise component from  $\text{Normal}(0, \sqrt{(1-h^2)V_{P[z]}})$ , where  $\bar{z}_{t=0}$  is the initial mean trait value,  $h^2$  is the initial trait heritability and  $V_{P[z]}$  the initial phenotypic variance. The trait value is then obtained by summing the genetic and noise components, and in the case of  $d_{max}$ , back-transforming the sum from the logit scale:  $d_{max} = \text{logit}^{-1}(a_{[d_{max}]} + r_{[d_{max}]})$ ,  $\alpha = a_{[\alpha]} + r_{[\alpha]}$ ,  $\beta = a_{[\beta]} + r_{[\beta]}$ .
- we calculate secondary individual-level statistics from  $d_{max}$ ,  $\alpha$  and  $\beta$  (see the Dispersal submodel description below).

## Input data

The model is self-sufficient and does not use external input data to represent time-varying processes.

## Submodels

**Dispersal:** during the dispersal phase, an individual leaves its natal patch with a probability  $d$ , which depends on individual traits and local population size  $N$  as measured at the start of the dispersal phase (here expressed relative to the constant  $K$ ) based on Kun and Scheuring (2006)’s model (see also Travis et al., 2009):

$$d_N = \frac{d_{max}}{1 + \exp(-\alpha(\frac{N}{K} - \beta))}.$$

Compared to other dispersal models (such as those reviewed in Hovestadt et al., 2010), this three-parameter model has the advantage of flexibility, can model a wide variety of realistic dispersal curves, and allows for both negative and positive density-dependent dispersal. In addition, all three parameters have an ecologically relevant interpretation:

- $d_{max}$  is the maximal dispersal rate, and can be seen as a measure of dispersal capacity. Note that depending on the other parameters,  $d_{max}$  may not be reachable at any of the population sizes actually experienced during the simulation.
- $\alpha$  is the slope of the dispersal-density relationship and describes the “strength” of the response to population density (relative to  $d_{max}$ ). Whether  $\alpha$  is positive or negative determines whether dispersal increases or decreases with population size. Depending on  $\beta$ ,  $\alpha$  may or may not influence meaningfully the actual dispersal strategy at the population sizes experienced during the simulation.
- $\beta$  is the inflection point of the dispersal function, i.e. the density at which  $d = 0.5 \times d_{max}$ . It can be interpreted as a response threshold, i.e. how high (or low) density must get for the individual to substantially alter its dispersal response. We allow  $\beta$  to be negative; this can be interpreted as individuals being so sensitive to density that they already are close to their high density dispersal behaviour at low densities. For our purpose, this is the only practical way the model can produce density-independent functions where  $d \approx d_{max}$  (as setting  $\alpha$  to 0 actually sets  $d$  to be constant, but  $= 0.5 \times d_{max}$ ). Another way is theoretically possible: allowing  $\beta$  to be close to 0 or  $K$  but positive, and  $|\alpha|$  to be so high (for a given  $K$ ) that dispersal goes from 0 to  $d_{max}$ , or the opposite, between  $N = 0$  and  $N = 1$  (as in e.g. Travis et al., 2009). However, due to how  $\alpha$  influences the shape of the dispersal function, Normal distributions of initial  $\alpha$  that allow for such high  $|\alpha|$  would be strongly biased against shallower slopes (see **Supplementary Material S2**).

Following the terminology in Cote et al (2017), variation in  $d_{max}$  can be interpreted as encoding variation in dispersal enhancing or enabling traits, while variation in  $\alpha$  or  $\beta$  corresponds to variation in dispersal matching traits.

Once we know the  $d_{max}$ ,  $\alpha$  and  $\beta$  of an individual, we additionally calculate three values at the individual-level:

- $d_0$ , the hypothetical dispersal rate at  $N = 0$ . The theoretical distinction between pulled and pushed expansions hinges on whether expansion move as fast as expected from  $d_0$  or faster (e.g. Birzu et al., 2019).
- $d_K$ , the expected dispersal rate at  $N = K$ .
- A measure of the strength of density-dependence  $\Delta_{K-0} = d_K - d_0$ .

We note that the model can easily be modified to add instructions for other metrics describing additional aspects of the shape of the density-dispersal function.

**Reproduction:** Each adult individual still living during the reproduction stage produces  $F$  offspring, with  $F \sim \text{Poisson}(\lambda)$  and the average offspring number  $\lambda$  depending on local population size  $N$  based on a Ricker model:

$$\lambda_N = e^{r_N}, r_N = r_0(1 - N/K),$$

where  $r_0$  is the hypothetical *per capita* growth rate at  $N = 0$ .

Parent transmit their genetic values (dispersal-related:  $a_{[d_{max}]}$ ,  $a_{[\alpha]}$ ,  $a_{[\beta]}$  and neutral:  $\gamma$ ) directly to their offspring without any mutation. Offspring then draw random values of noise components  $r_{[d_{max}]}$ ,  $r_{[\alpha]}$ ,  $r_{[\beta]}$  from  $\text{Normal}(0, \sqrt{V_{R[z]}})$ , where  $z$  is the trait in question. For each trait  $z$ , the “random noise” variance  $V_R$  is equal to  $(1 - h^2)V_{P[z]}$ , where  $h^2$  is the *initial* heritability at  $t = 0$  and  $V_P$  the *initial* phenotypic variance.

**Observation:**

The code estimates and reports a variety of summary variables at the patch level, typically means and variances of individual-level traits, as well as counts of individuals, and can easily be modified to add more. Of potential interest are the following:

- the means of  $d_{max}$ ,  $d_0$ ,  $\Delta_{K-0}$  for all individuals born in a patch.
- the variances of the genetic components  $a_{[d_{max}]}$ ,  $a_{[\alpha]}$ ,  $a_{[\beta]}$  for all individuals born in a patch.
- population sizes  $N$  pre- and post-dispersal phase.
- the frequencies of the two neutral alleles in a patch, both pre- and post-dispersal phase.

## S2 - Effect of the magnitude of initial variation in $\alpha$ on density dependence

In the ODD description above, we briefly discuss how allowing for negative  $\beta$  is the only way we have to create mostly flat dispersal-density function where dispersal is close to  $d_{max}$ . We briefly explain that one seeming alternative, forcing  $\beta$  to stay  $\geq 0$  and allowing very large  $|\alpha|$  values so that dispersal goes from 0 to close to  $d_{max}$  between  $N = 0$  and  $N = 1$ , is not viable for our purposes. We expand this argument here.

Using very large  $\alpha$  means we’d need the initial trait distribution to contain both these very large  $\alpha$  (positive and/or negative) *and*  $\alpha$  close to 0, for evolution to be possible (in the absence of mutation at least). It’s easy to demonstrate that distributions that fulfill this requirement are actually biased towards very sharp density-dispersal functions. If we assume  $K = 250$  as in our simulations, then  $\alpha$  close to 1000 are needed to generate one of these nearly flat functions (**Fig. S2.1**):

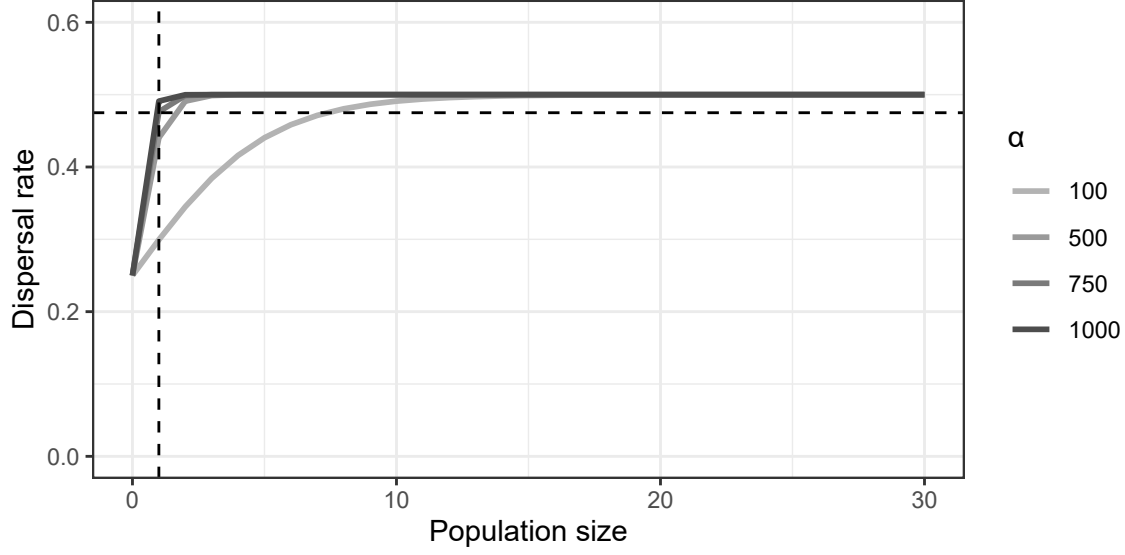


**Figure S2.1.** Example of how one can produce a functionally flat density-dispersal function using a very sharp slope  $\alpha$  ( $d_{max} = 0.5$ ,  $\beta = 0$ ). The dashed lines mark  $N = 1$  (vertical) and  $d_N = 0.95 \times d_{max}$  (horizontal).

So, even after setting  $\beta$  at 0, we still need  $\alpha$  in the neighbourhood of 1000 to be able to produce such shapes (when, as a reminder,  $\alpha = 6$  is needed to get a slope that takes a population increase of  $K$  individuals to go from 5% to 95% of  $d_{max}$ , so a reasonably shallow, but not too shallow function). An initial distribution of  $\alpha$  of  $\text{Normal}(0, 500)$  would hit these extreme  $\alpha$  with low but non-negligible probabilities. And we know (see main text) that  $6/|\alpha|$  approximately expresses (in units of  $K$ ) how sharp the increase in dispersal with density is. Let's have a look at the distribution of  $6/|\alpha|$  implied by  $\alpha \sim \text{Normal}(0, 500)$  (**Fig. S2.2**):

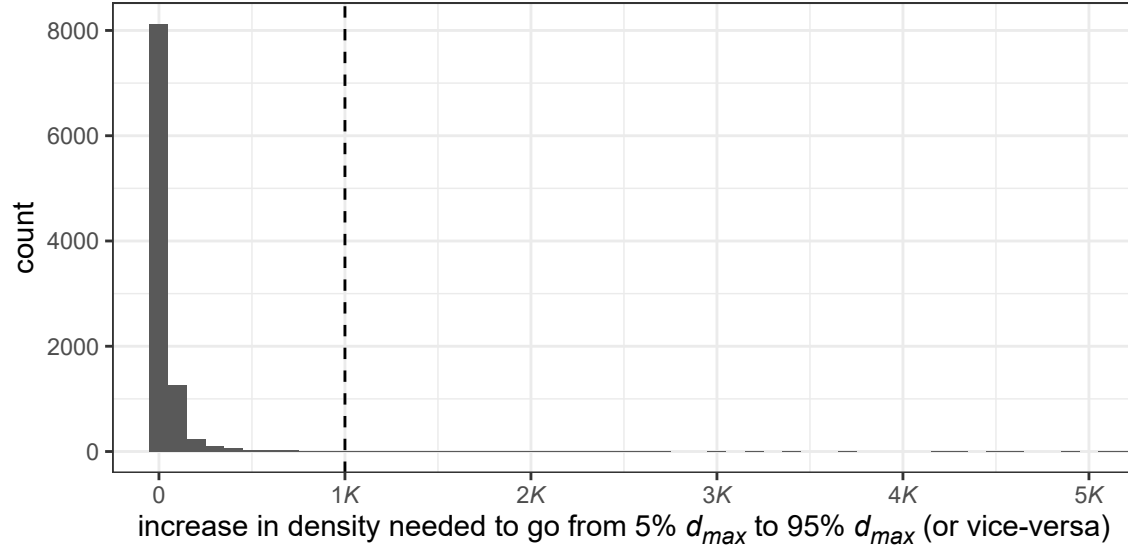


**Figure S2.2.** Distribution of the increases in density needed to go from 5% of  $d_{max}$  to 95%, assuming  $\alpha \sim \text{Normal}(0, 500)$ . Histogram drawn based on 10000 samples, the  $x$  axis is cut at 5K for better visualisation.

We can see that this initial distribution of  $\alpha$  would mostly only allow sharp slopes, that take less than 20-50%K to go from (nearly) 0 to (nearly)  $d_{max}$ , and shallower slopes would only be present at much lower

frequencies. This is not a choice that is ecologically sound in our opinion; hence why we rejected “extreme  $\alpha$ ” as a method to generate  $d_N \approx d_{max}$  flat functions.

### S3 - Distribution of the replicates that failed to expand

Exploring data shows that all 109 replicates that either went extinct or otherwise failed to expand had low fecundity ( $r_0 = \log(1.5)$ ) and high dispersal mortality ( $m = 0.9$ ). Looking into this subset of the data in more detail (**Fig. S3.1**), we find that:

- most failed expansions are in replicates where evolution is not allowed. This suggests a role of evolutionary rescue;
- failed expansions all have negative initial density-dependence  $\Delta_{K-0}$ ;
- however, this does not reduce the available range of density-dependence for analyses that rely on only successful expansions, and most replicates with  $\Delta_{K-0} < 0$  successfully expand.

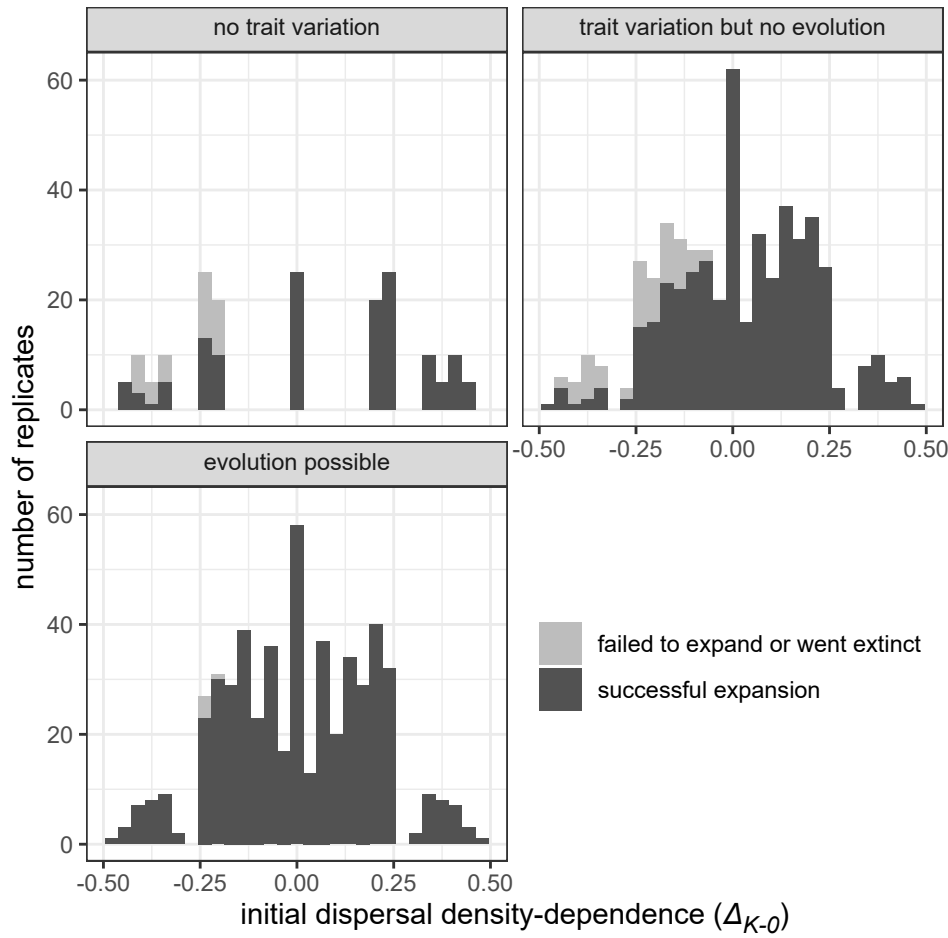


**Figure S3.1.** Distribution of the simulation replicates based on their initial density-dependence  $\Delta_{K-0}$  and on whether they successfully expanded by  $t = 120$  or went extinct/remained stuck at  $x = 0$ . Only replicates with low fecundity ( $r_0 = \log(1.5)$ ) and high dispersal mortality ( $m = 0.9$ ) are displayed, since expansions under other conditions where all successful.

## S4 - How do we define the “range front”?

We are interested in how traits at the front of the expansion are shaped by, and shape, the expansion process. To do that right, we need an operational definition of what is the front. A “traditional” one is the range of patches where a density gradient is seen, i.e. where population density has not yet reached its equilibrium (e.g. Gandhi et al., 2016; Lewis et al., 2016).

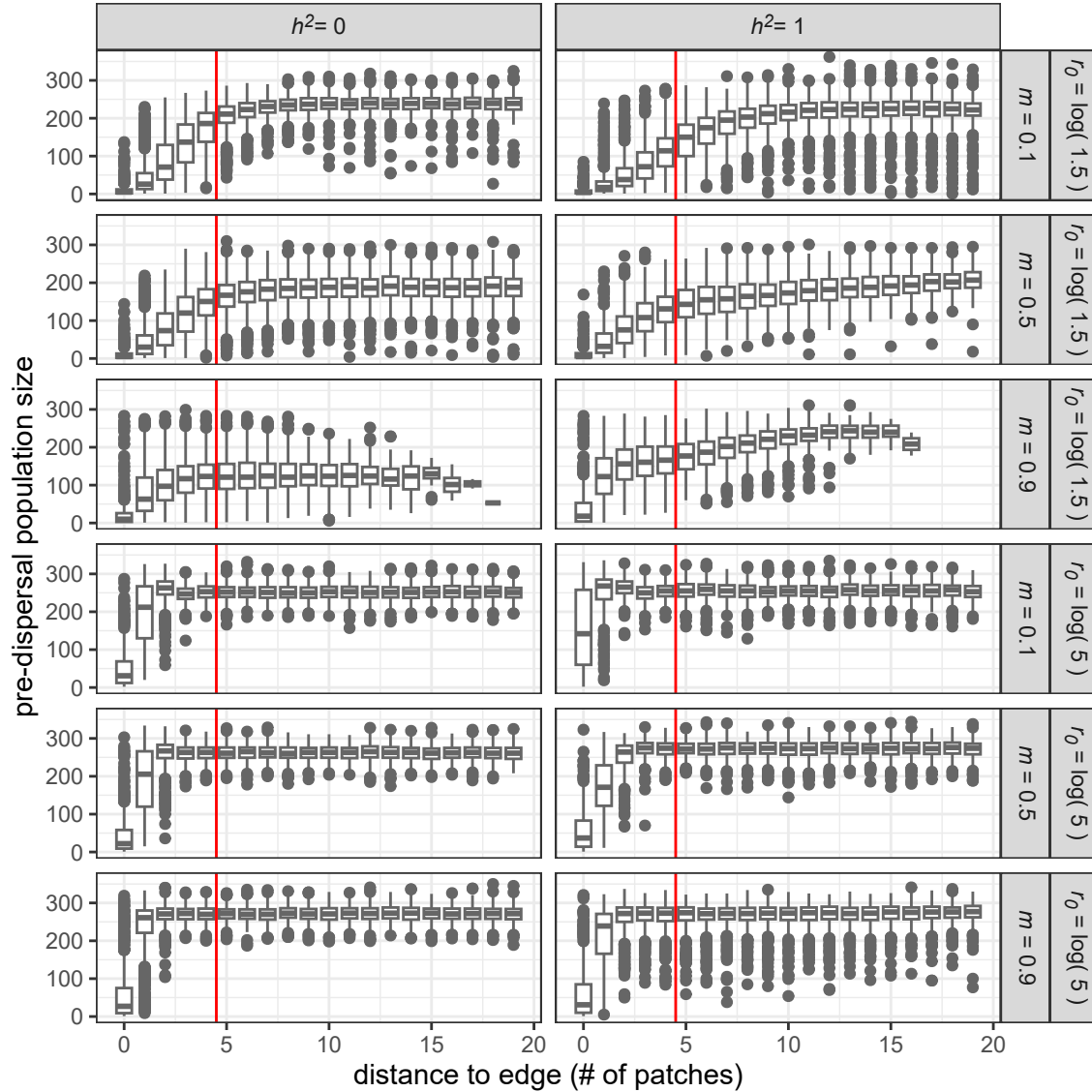


**Figure S4.1.** Predispersal population size as a function of distance to the range edge (only populations up to 20 patches from the edge at the time of sampling included). The vertical line separate the 5 patches closest from the edge from the others.

We can see **Fig. S4.1** that a threshold where we consider the 5 patches closest from the edge (edge patch included) as belonging to the range front is a good compromise that works across conditions. Narrower fronts would probably work for the high fecundity scenarios, but would not work for the low fecundity ones. In addition, a narrower threshold would limit the number of individuals included, reducing the precision of our trait means, while a wider one would lead us to fronts that are dominated by what are clearly non-front patches when fecundity is high.



## S5 - Genetic variation at the end of the simulated expansions

For all three dispersal traits, a very large majority of replicates have lost most if not all of their genetic variance by  $t = 120$  (Figs S5.1, S5.2 and S5.3), meaning there is limited to no potential for further evolution should the simulations run for longer. Note that Figs S5.1 to S5.3 may still overstate the remaining potential for evolution: indeed, disruptive selection may lead to replicates where the final variances are still high, even higher than initial variances, and yet there are no further opportunities for selection.

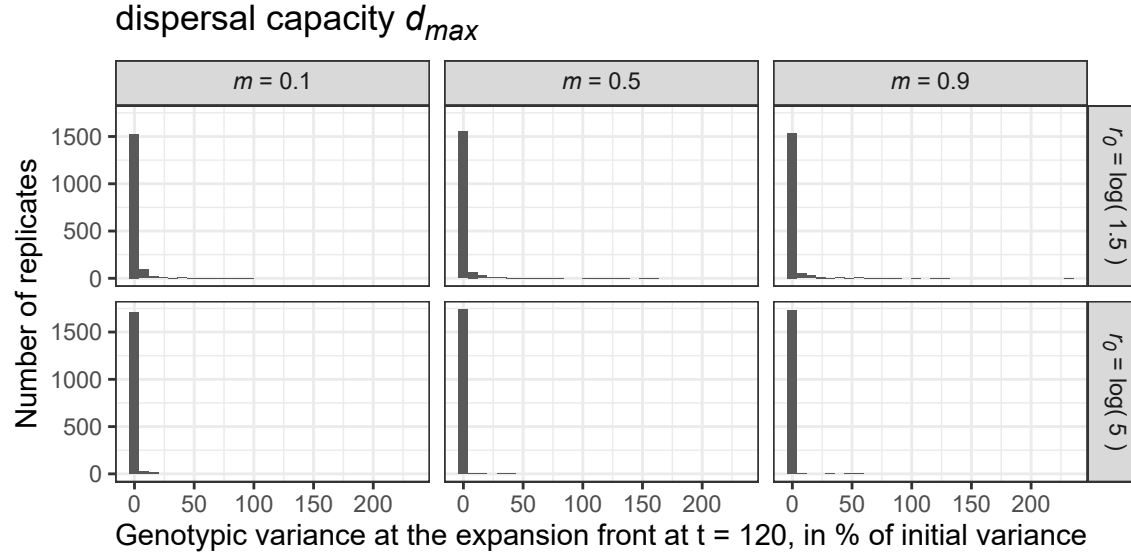


**Figure S5.1.** Distribution of the remaining genetic variance in  $\text{logit}(d_{max})$  at the expansion front at the end of the expansion. The values displayed are weighted averages of the patch-level variances, with the front defined as in S4. Only replicates that started with non-zero genetic variance in  $\text{logit}(d_{max})$  are displayed.

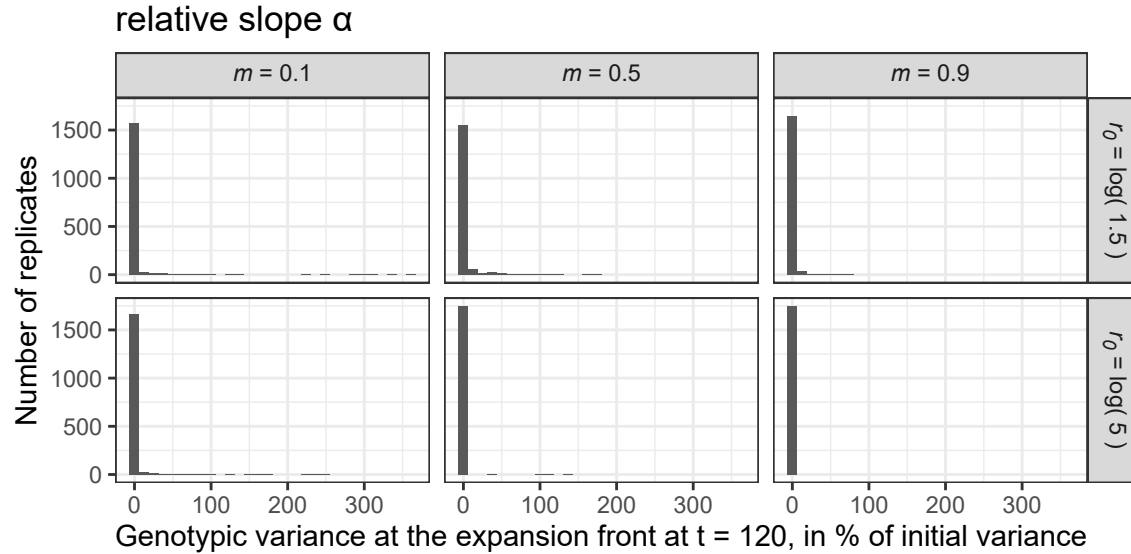


**Figure S5.2.** Distribution of the remaining genetic variance in the relative slope  $\alpha$  at the expansion front at the end of the expansion. The values displayed are weighted averages of the patch-level variances, with the front defined as in S4. Only replicates that started with non-zero genetic variance in  $\alpha$  are displayed.

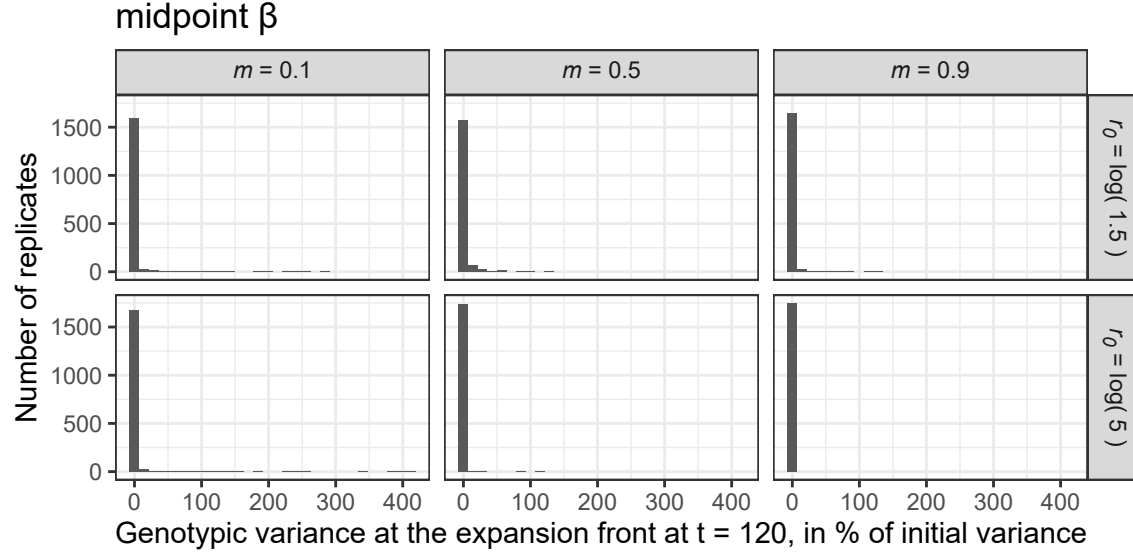


**Figure S5.3.** Distribution of the remaining genetic variance in the midpoint  $\beta$  at the expansion front at the end of the expansion. The values displayed are weighted averages of the patch-level variances, with the front defined as in **S4**. Only replicates that started with non-zero genetic variance in  $\beta$  are displayed.

## S6 - Velocities in replicates with evolution, split based on whether $d_{max}$ can evolve or not

Here we provide versions of **Fig. 4** of the main text, but this time by separating replicates where the maximal dispersal rate can (**Fig. S6.1**) or cannot (**Fig. S6.2**) evolve. We see that the qualitative conclusions we present in the main text apply to both subsets similarly.

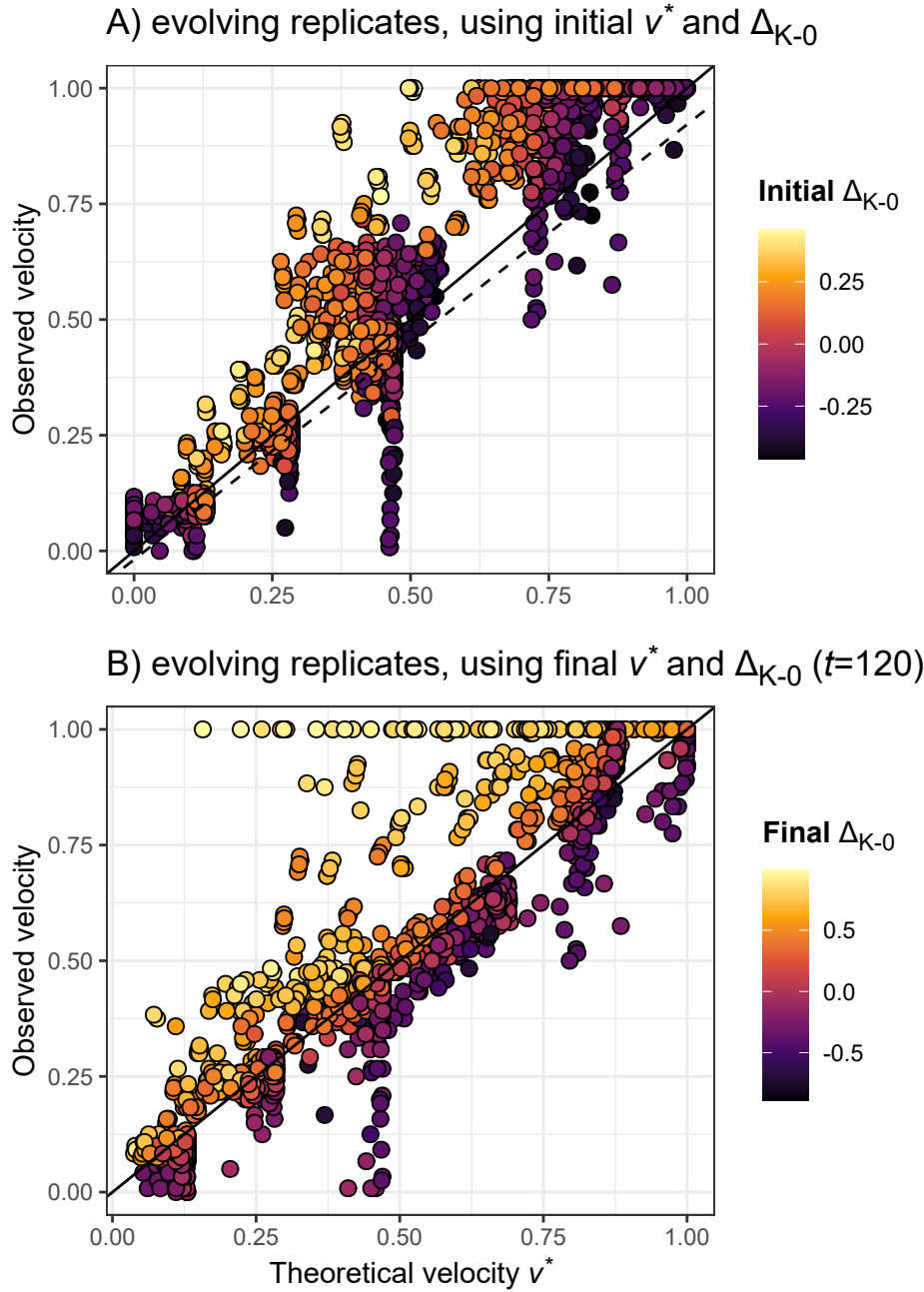


**Figure S6.1.** Relationship between observed expansion velocities and expected theoretical velocities  $v^*$ , in expansions where the maximal dispersal rate  $d_{max}$  was allowed to evolve (whether or not density-dependence traits were allowed to). In (A),  $v^*$  and dispersal density-dependence  $\Delta_{K-0}$  are both calculated based on the initial distribution of dispersal traits, as in **Fig. 3** of the main text; in (B) they are instead calculated based on traits at the range front after evolution, at the end of the simulated expansion. Each replicate is coloured according to its value of dispersal density-dependence (note the different scales in (A) and (B)). The full straight lines correspond to  $y = x$ , the dotted line in (A) is the linear regression from **Fig. 3B** of the main text, i.e. for the replicates with  $\Delta_{K-0} = 0$  only in the absence of evolution.

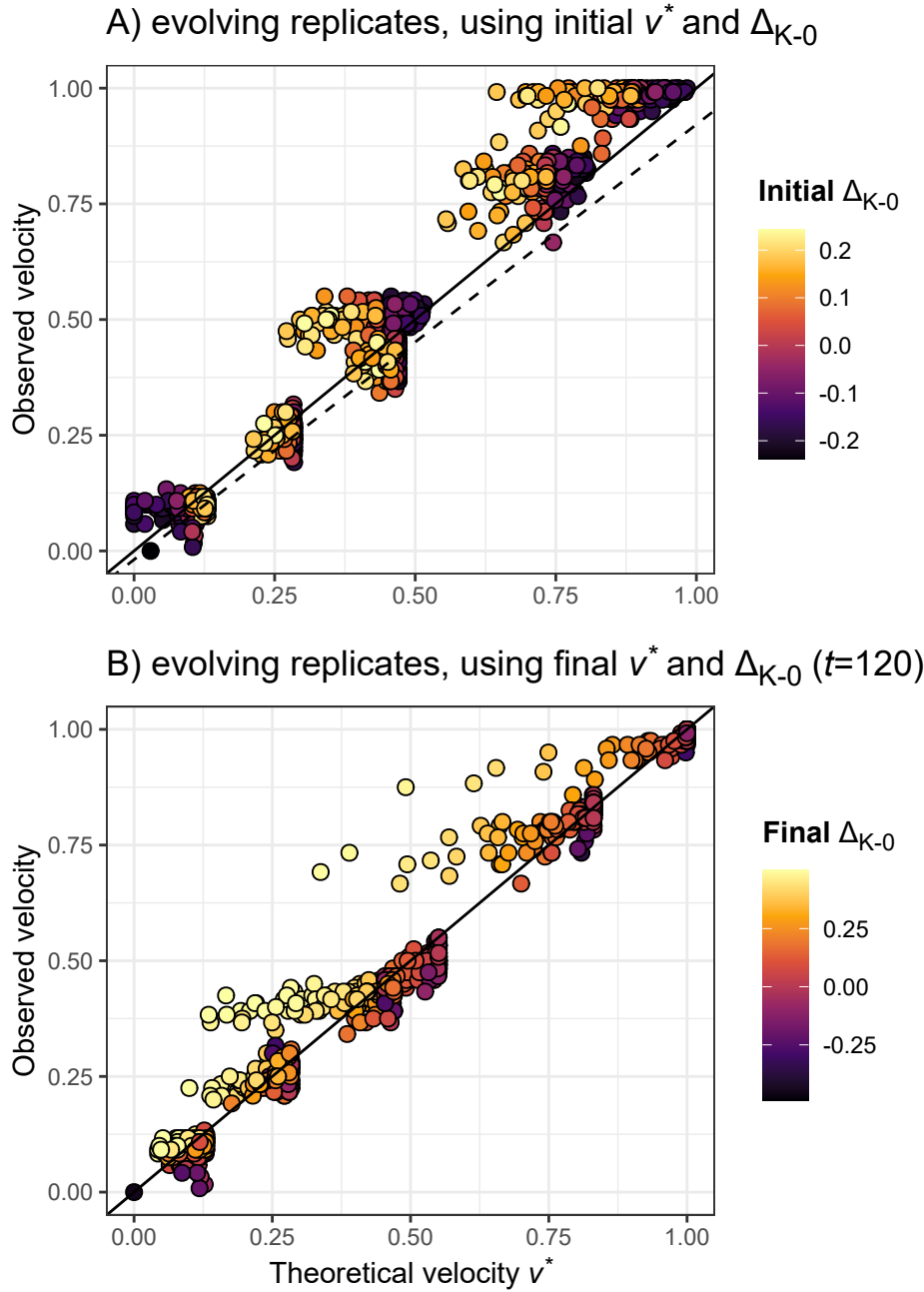


**Figure S6.1.** Relationship between observed expansion velocities and expected theoretical velocities  $v^*$ , in expansions where evolution was possible but only density-dependence traits ( $\alpha$  and  $\beta$ ) were allowed to evolve. Legend is otherwise identical to **Fig. S6.2**.

## S7 - Relationship between velocity and density-dependence when costs are high and fecundity low

We reproduce here a subset of the main text **Fig. 3**, focusing only on replicates with low fecundity and high dispersal mortality (**Fig. S7.1**). We show that in this subset, and contrary to the whole dataset, we do not find the relationship between expansion velocity and density-dependence that is expected from theory; that

is, high  $\Delta_{K-0}$  do not lead to consistently higher velocities than expected from their  $v^*$ . The absence of a key pattern from pushed expansion theory is to put in perspective with a similar absence regarding genetic diversity (see main text **Fig. 5**).

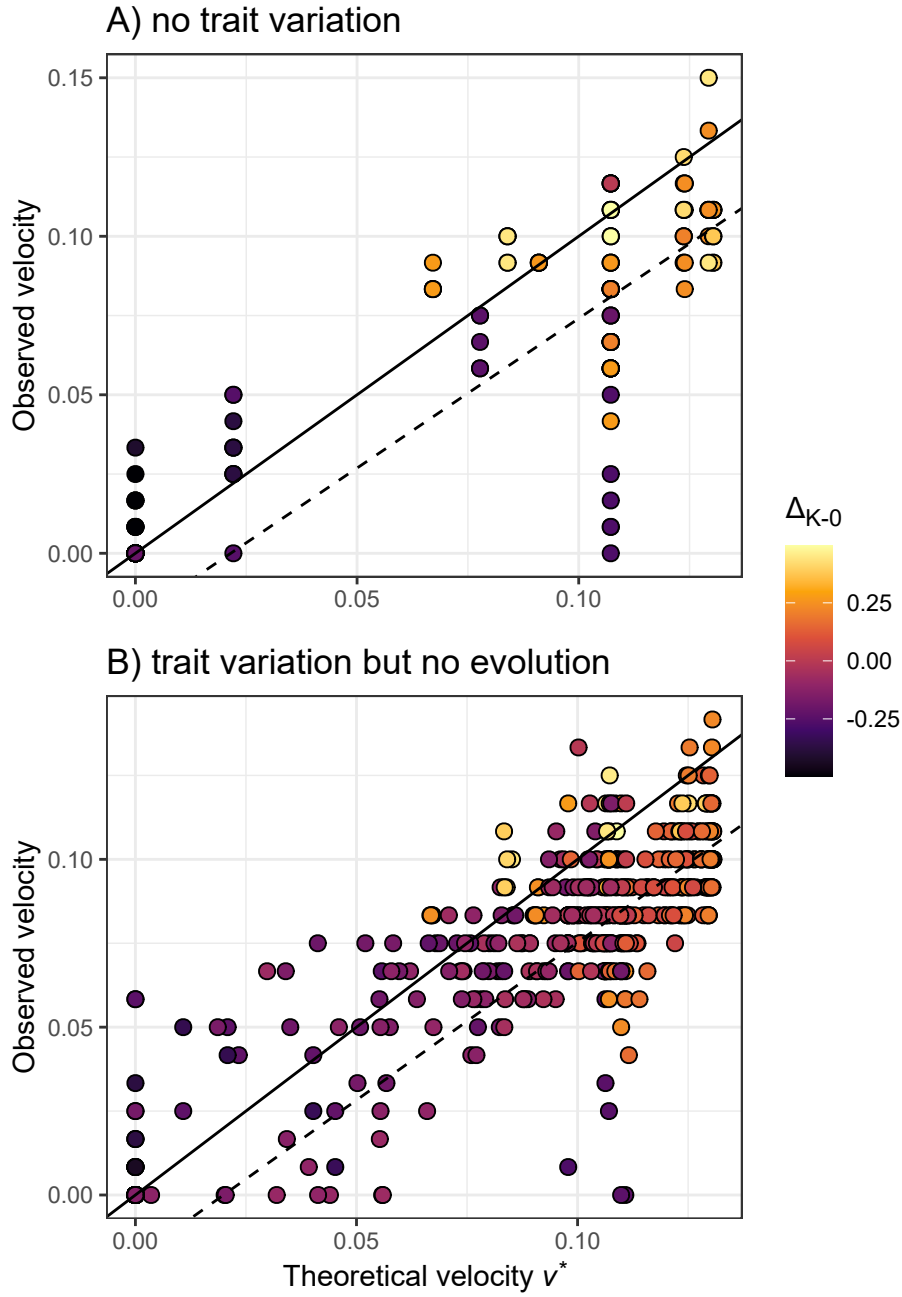


**Figure S7.1.** Relationship between observed expansion velocities and expected theoretical velocities  $v^*$ , in the absence of trait evolution and for replicates with low fecundity ( $r_0 = \log(1.5)$ ) and high dispersal mortality ( $m = 0.9$ ). Each replicate is coloured according to its value of dispersal density-dependence. The full straight lines correspond to  $y = x$ , the dotted line are linear regressions for the replicates with  $\Delta_{K-0} = 0$  only (using all fecundity and mortality values, as in **Fig.3** of the main text).

## References

- Birzu, G., Hallatschek, O., & Korolev, K. S. (2018). Fluctuations uncover a distinct class of traveling waves. *Proceedings of the National Academy of Sciences*, 115(16), E3645–E3654. <https://doi.org/10.1073/pnas.1715737115>
- Birzu, G., Matin, S., Hallatschek, O., & Korolev, K. S. (2019). Genetic drift in range expansions is very sensitive to density dependence in dispersal and growth. *Ecology Letters*, 22(11), 1817–1827. <https://doi.org/10.1111/ele.13364>
- Cote, J., Bestion, E., Jacob, S., Travis, J., Legrand, D., & Baguette, M. (2017). Evolution of dispersal strategies and dispersal syndromes in fragmented landscapes. *Ecography*, 40(1), 56–73. <https://doi.org/10.1111/ecog.02538>
- Erm, P., & Phillips, B. L. (2020). Evolution transforms pushed waves into pulled waves. *The American Naturalist*, 195(3), E87–E99. <https://doi.org/10.1086/707324>
- Gandhi, S. R., Yurtsev, E. A., Korolev, K. S., & Gore, J. (2016). Range expansions transition from pulled to pushed waves as growth becomes more cooperative in an experimental microbial population. *Proceedings of the National Academy of Sciences*, 113(25), 6922–6927. <https://doi.org/10.1073/pnas.1521056113>
- Hovestadt, T., Kubisch, A., & Poethke, H.-J. (2010). Information processing in models for density-dependent emigration: A comparison. *Ecological Modelling*, 221(3), 405–410. <https://doi.org/10.1016/j.ecolmodel.2009.11.005>
- Kun, Á., & Scheuring, I. (2006). The evolution of density-dependent dispersal in a noisy spatial population model. *Oikos*, 115(2), 308–320. <https://doi.org/10.1111/j.2006.0030-1299.15061.x>
- Lewis, M., Petrovskii, S. V., & Potts, J. (2016). *The mathematics behind biological invasions*. Springer International Publishing. <https://doi.org/10.1007/978-3-319-32043-4>
- Travis, J. M. J., Mustin, K., Benton, T. G., & Dytham, C. (2009). Accelerating invasion rates result from the evolution of density-dependent dispersal. *Journal of Theoretical Biology*, 259(1), 151–158. <https://doi.org/10.1016/j.jtbi.2009.03.008>